Optimal realization of arbitrary forces in a magnetic stereotaxis system. *

David C. Meeker
Eric H. Maslen
Rogers C. Ritter
Francis M. Creighton

Abstract

Very small implanted permanent magnets guided by large electromagnetic coils have been proposed previously as a method for delivering hyperthermia to or guiding catheters through brain tissue. This procedure is termed "magnetic stereotaxis." Early efforts employed a single coil on a movable boom, a design that proved logistically difficult to use on human patients. The present work deals instead with a design where several stationary coils are employed to develop a force on the implanted magnet. The coil current-to-force relationship is developed for this type of machine, and several optimal solutions for realizing an arbitrary static force are presented for various constraints on the orientation of the implanted permanent magnet. Costs of the different solutions are compared in several examples using a mathematical model based on the Magnetic Stereotaxis System (MSS) developed by Stereotaxis, Inc., the University of Virginia, and Wang NMR.

1 Introduction

Magnetic stereotaxis is a novel therapeutic methodology for the treatment of brain tumors and other neurological problems. The fundamental idea of magnetic stereotaxis is that large electromagnetic coils can be used to guide a small piece of implanted permanent magnetic material (a "magnetic seed") along some arbitrary trajectory through brain tissue. Incidental damage is reduced by selecting a path that avoids important brain structures. Once the seed has been maneuvered into a tumor, the seed is heated inductively by high-frequency magnetic fields. This heating results in highly localized cell death. By successive movements and heating, a tumor could be destroyed with little damage to the surrounding tissue [1]. Alternatively, the magnetic seed could be used to guide the tip of a catheter. This catheter would then be used to deliver drug treatments directly to sites inside the brain [2][3].

Previous efforts in magnetic stereotaxis used a single movable coil to act upon the implanted magnet. This arrangement proved successful in experiments using live dogs [4]. Scaling the device to work on humans, however, has been difficult. The size and weight of the required coil interfere with the necessary bi-planar fluoroscopes and make precision manipulation impractical in an operating room environment [2] [5].

Subsequent efforts have focused, instead, upon an arrangement of stationary coils, as shown in Figure 1. Since the coils are operating in a region of uniform, linear magnetic permeability, the fields of the coils are additively superimposed upon one another. With a proper selection of currents, a wide range of forces can be applied to the magnetic seed. One such device, the Magnetic Stereotaxis System (MSS) developed by the University of Virginia, Stereotaxis, Inc., and Wang NMR, Inc., has been built and is currently in the process of testing [6] [7]. This device uses a roughly cubic array (or "helmet") of six superconducting coils.

Several problems preclude the closed-loop control of machines such as the MSS. First, the superconducting coils of such a machine have a large inductance. Second, the currents inside the coils cannot be changed faster than a certain rate (making changes in current difficult and costly), or the coils will become heated and

*Copyright 1996 IEEE. Personal use of this material is permitted. However, permission to reprint/republish this material for advertising or promotional purposes or for creating new collective works for resale or redistribution to servers or lists, or to reuse any copyrighted component of this work in other works must be obtained from the IEEE. Published IEEE *Transactions on Magnetics*, VOL. 32, NO. 2, March 1996, pp. 320–328.

Nomenclature

’	Denotes transpose.
a	Magnetic vector potential.
b	Vector flux density.
b	Column matrix of flux density components.
B	Current-to-flux density matrix.
c	Transformed coil currents.
C	Cost function.
d	Column matrix of desired force and field.
D	Matrix of flux density derivatives.
e	Unit vector defining frame aligned with desired force.
f	Vector force on dipole.
f	Column matrix of force components.
G	Dipole constraints matrix.
i	Coil currents.
j	Vector current density.
K	Current-to-force matrix.
m	Vector dipole moment.
M	Spherical seed current-to-force matrix.
m	Column matrix of dipole moment components.
n	Unit vector defining helmet-fixed reference frame.
p	Position vector.
P	Identity matrix lacking last column.
r	Vector from differential current volume to field point.
t	Torque on dipole.
T	Transformation matrix.
U,V,W	Sing. val. decomposition. of G.
v	Unrealizable vector of singular G.
x,y,z	Components of **p**.
α	Flux density to force ratio.
ε	force – flux misalignment angle.
γ	Magnitude of **m** (const. for a given seed).
λ	Lagrange multiplier.
μ	Magnetic permeability.

lose their superconductivity – a catastrophic failure known as “quench”. Lastly, the tissue through which the seed moves is moderately heterogeneous, leading to significant model uncertainty. Due to these difficulties, an open-loop control scheme has been chosen.

In the open-loop control scheme, movement of the seed proceeds in small steps. The steps are short enough that variations in the current-to-force relationships due to seed movement can be ignored and the effects of modeling errors remain small. The static current solutions addressed in this work then can be assumed to apply over the entire length of the seed’s movement. The scheme consists of first determining a set of currents which applies a force in the desired direction of motion. The magnitude of this set of coil currents is then ramped up and down once, resulting in a small movement of the seed. Magnitude and duration of the current ramping are chosen so that the seed will typically move a centimeter or less during each pulse. After each pulse, the seed’s position is determined by fluoroscopes and is assessed by the operator. A new force direction is then chosen to continue progress toward the ultimate target. A similar open-loop scheme consisting of successive small seed motions has been used successfully in surgical trials of the single movable coil MSS [4] and in on-axis movements of the six-coil MSS [6].

Previously, the control scheme lacked predetermined constraints on the selection of currents leading to a force in the desired direction of movement. Selection therefore proceeded somewhat heuristically, complicating the machine’s operation. The present work addresses the problem of the selection of currents needed to realize an arbitrary force in the general class of stationary-coil magnetic stereotaxis systems. The current-to-force relationship for such devices is first characterized. Three classes of solutions for the currents needed to produce an arbitrary force are presented. For convenience, a six-coil MMS is specifically addressed; however, these solutions can be easily extended to a machine with more than six coils. These solutions assume different constraints on the orientation of the implanted magnet relative to the direction of the desired force. Seed orientation is especially important when a catheter is being pulled; misalignment can cause unacceptable damage to brain tissue during seed motion. It will be shown that the problem is usually underconstrained, implying the existence of many solutions for any given force orientation. An optimal solution is chosen in each case on the basis of a quadratic measure of the coil currents. Solutions under each set of alignment

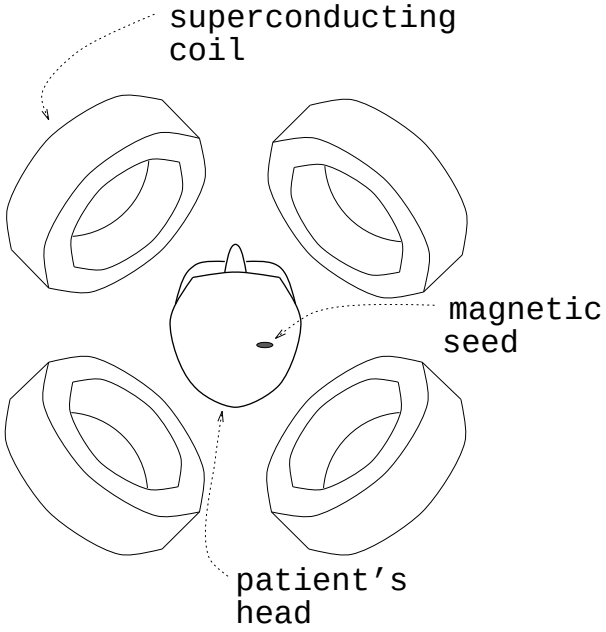

Figure 1: Schematic of multi-coil MSS.

constraints are then demonstrated through several illustrative examples using the specific configuration of the Magnetic Stereotaxis System.

2 Governing Dipole Equations

Since the dimensions of the permanent magnet seed are very small compared to the size of the superconducting coils, the seed can be idealized as a point dipole. The magnetic properties of the seed are summarized by the seed's dipole moment, **m**. The direction of this vector is the same as the direction of magnetization in the seed. The magnitude of **m** is the product of the magnetization and volume of the seed.

Derivation of the forces and torques on a dipole due to an applied magnetic field can be found in the literature [8]. Defining **p** as a position vector locating the seed relative to the center of the helmet, the force on the seed is

$$\mathbf{f}(\mathbf{p}) = \nabla(\mathbf{m} \cdot \mathbf{b}(\mathbf{p})) \tag{1}$$

and the torque is

$$\mathbf{t}(\mathbf{p}) = \mathbf{m} \times \mathbf{b}(\mathbf{p}) \tag{2}$$

3 Formulation of Current-to-Force Relationships

Equations (1) and (2) specify the force and torque respectively on the dipole seed, but they do not imply any particular basis in terms of which these vectors are represented. A computationally useful form of these equations can be obtained by defining a basis of orthogonal vectors $\mathbf{n}_1, \mathbf{n}_2$ and $\mathbf{n}_3$ that are fixed at the center of the helmet. With these vectors, define

$$\begin{array}{lcl} \mathbf{p} & = & x\mathbf{n}_1 + y\mathbf{n}_2 + z\mathbf{n}_3 \\ \mathbf{m} & = & m_1\mathbf{n}_1 + m_2\mathbf{n}_2 + m_3\mathbf{n}_3 \\ \mathbf{f} & = & f_1\mathbf{n}_1 + f_2\mathbf{n}_2 + f_3\mathbf{n}_3 \\ \mathbf{b} & = & b_1\mathbf{n}_1 + b_2\mathbf{n}_2 + b_3\mathbf{n}_3 \end{array} \tag{3}$$

Since **m** is not a function of **p**, (1) can be written in matrix form as

$$f_1 = m' \frac{\partial b}{\partial x}$$

$$f_2 = m' \frac{\partial b}{\partial y} \tag{4}$$
$$f_3 = m' \frac{\partial b}{\partial z}$$

where $(')$ denotes transpose.

Equation (4) defines the field-to-force relation in a particular reference frame, but the connection between coil currents and the magnetic field (b) must still be defined. Since the permeability of the seed is very close to that of free space, it is appropriate to characterize the field at a point as a linear superposition of field contributions created by each of the six coils. Furthermore, the contribution of any particular coil is linearly proportional to the current in that coil. The relationship between coil current and field can then be concisely represented in matrix notation as

$$b(x,y,z) = B(x,y,z)\, i \tag{5}$$

where i is a column matrix of coil currents and B is a 3×6 matrix dependent on seed position. The k^{th} column B represents the contribution of the k^{th} coil to the field at (x,y,z) in response to a unit of current in the coil.

Spatial derivatives of the field also follow the same rule of superposition. Coil currents are related to these derivatives by the differentiation of (5):

$$\frac{\partial b}{\partial w} = \left[\frac{\partial B(x,y,z)}{\partial w} \right] i \qquad \text{where} \qquad w = x,y,z \tag{6}$$

Defining

$$D_1 = \frac{\partial B}{\partial x}; \qquad D_2 = \frac{\partial B}{\partial y}; \qquad D_3 = \frac{\partial B}{\partial z} \tag{7}$$

and referring to (4), a particular force component is

$$f_j = m' D_j i \tag{8}$$

For a given dipole orientation, all force components can be collected into the expression

$$f = K(\mathbf{p}, \mathbf{m})\, i \tag{9}$$

where

$$K(\mathbf{p}, \mathbf{m}) = \begin{bmatrix} m' D_1 \\ m' D_2 \\ m' D_3 \end{bmatrix} \tag{10}$$

4 Determination of the Magnetic Field

The determination of the elements of the B and D matrices is not a trivial task and deserves some comment. In the most general case, finding the magnetic field produced by a coil involves solving Maxwell's equations for the special case of magnetostatic fields (summarized, for example, in [9]). These equations are:

$$\frac{1}{\mu} \nabla \times \mathbf{b} = \mathbf{j} \tag{11}$$

$$\nabla \cdot \mathbf{b} = 0 \tag{12}$$

where $\mathbf{j}$ is vector current density. By defining $\mathbf{b}$ in terms of vector potential $\mathbf{a}$ as

$$\mathbf{b} = \nabla \times \mathbf{a} \tag{13}$$

equations (11) and (12) are both satisfied if the vector potential satisfies

$$\frac{-1}{\mu} \nabla^2 \mathbf{a} = \mathbf{j} \tag{14}$$

The MSS, however, is specifically built only of materials that have a magnetic permeability very near that of free space. In the case of uniform permeability μ_o, the contribution of a differential volume of current to the vector potential has the solution

$$d\mathbf{a} = \frac{\mu_o}{4\pi}\frac{\mathbf{j}}{|\mathbf{r}|}dV \tag{15}$$

where $\mathbf{r}$ is a position vector from the differential current element to the point of interest. The current density is a linear function of current i flowing through the coil.

$$\mathbf{j} = i\hat{\mathbf{j}} \qquad \text{where} \qquad |\hat{\mathbf{j}}| = \frac{\text{(\# of turns)}}{\text{(coil cross-sectional area)}} \tag{16}$$

Flux density in terms of coil current is found by differentiating according to (13) and substituting from (16).

$$d\mathbf{b} = \frac{\mu_o i}{4\pi}\left(\frac{\hat{\mathbf{j}}\times\mathbf{r}}{|\mathbf{r}|^3}\right)dV \tag{17}$$

This relation is commonly known as the Biot-Savart law. Equation (17) is numerically integrated over the volume of a coil to obtain the total field produced by the coil. Since (17) is a linear function of i, the field can be computed for a unit of current and then scaled for any other current. Because (14) is a linear differential equation, the total field can be determined by the superposition of the contributions from individual coils.

For efficient simulation of the MSS, the field is computed for grid of points at different radial and axial positions relative to the coil of interest. The field at a particular point is approximated by interpolating between known field values. If a suitably smooth interpolation and a fine enough grid is used, good approximations of the field derivatives can be obtained by differentiating the interpolation functions used to approximate the field.

5 Coil Current Solution

In this work, several forms of the i to f relation have been presented. These forms can be used in several different approaches to the problem of finding a set of currents that realizes a desired force on the seed. Three different scenarios will be considered; each approach considers different constraints on the seed orientation.

It is assumed for each configuration that the resistance of the seed to rotation is negligible, as has been observed experimentally [4] [7]. From (2), it can be noted that torque on the seed is zero only when $\mathbf{m}$ is aligned with $\mathbf{b}$. Furthermore, if $\mathbf{m}$ is parallel to $\mathbf{b}$, a small perturbation in $\mathbf{m}$ produces a torque that tends to re-align $\mathbf{m}$ and $\mathbf{b}$. The converse is true if $\mathbf{m}$ is antiparallel to $\mathbf{b}$. Since the seed is free to rotate, it will align with the only stable equilibrium orientation: $\mathbf{m}\,||\,\mathbf{b}$. Since there is a considerable threshold force that must be applied before translational motion begins, the seed is assumed to line up with $\mathbf{b}$ before any change in seed position occurs.

Generally, the seed is prolate, and the magnetization is aligned along the major axis. If a catheter is pulled, it is attached on one of the ends of the major axis. To minimize tissue damage, the field and force should be directed along the same line so that the seed presents the smallest possible profile and minimizes damage to tissue. Misalignment between the force and field vectors is called "skidding." Although no skidding at all is desirable, the currents required to realize this constraint are often unacceptably large. However, some skidding might be tolerable in exchange for lower current requirements. Three scenarios are therefore considered which impose different constraints on the amount of skidding allowed.

1. *Unlimited Skid Seed.* Since the seed attitude is not constrained, the desired force can be created with the dipole oriented in any position. A set of quadratic equations for the current-force relations arises. This configuration represents the most economical force for current case, since the best dipole orientation can be used.

2. *No Skid Seed.* The seed is prolate with the magnetization aligned along the major axis for this case. To cause the least damage to tissue as the seed moves, the dipole must be anti-parallel to the desired force direction.

3. *Limited Skid Seed.* The seed is again prolate. However, misalignment (skidding) bounded by a specified maximum angle is tolerated in exchange for a solution requiring lower currents.

5.1 Unlimited Skid Seed

The constraint that the dipole moment is aligned with the flux density field is written as

$$\mathbf{m} = \frac{|\mathbf{m}|}{|\mathbf{b}|}\mathbf{b} \tag{18}$$

Substituting from (5), the dipole moment in matrix notation is

$$m = \frac{\gamma B i}{\sqrt{i' B' B i}} \tag{19}$$

where $\gamma \equiv |\mathbf{m}|$. Combining (19) with the previously developed current to force relation (8) yields

$$f_j = \frac{\gamma i' B' D_j i}{\sqrt{i' B' B i}} \tag{20}$$

The numerator of (20) is quadratic in i. For ease of manipulation, it is preferable to manipulate quadratics in terms of operations on symmetric matrices. Any square matrix can be represented as the sum of a symmetric and an anti-symmetric matrix [11]. A quadratic formed from the anti-symmetric part is always zero; therefore, only the symmetric part of $B'D_j$ contributes to $i'B'D_j i$. Define M_j as the symmetric part of $B'D_j$:

$$M_j = \frac{1}{2}(D_j' B + B' D_j) \tag{21}$$

The force relations can now be written in terms of the symmetric matrices M_j and $B'B$:

$$f_j = \frac{\gamma i' M_j i}{\sqrt{i' B' B i}} \tag{22}$$

The problem of producing an arbitrary force on the seed is now that of finding an i that satisfies (22) for an arbitrary f. Generally, there exist many possible i that satisfy (22), since (22) represents three equations for six unknowns. This implies up to a three-dimensional manifold of solutions for i. More equations must be specified to rate the desirability of the valid solutions so that the most efficient solution is chosen.

One possible measure of solution quality is cost function C:

$$C = \frac{i' i}{\sqrt{i' B' B i}} \tag{23}$$

Minimization of C over the set of i that satisfies (22) is a trade-off between minimizing the currents needed to produce a force and strongly aligning the seed.

The problem of minimizing C over i subject to (22) can be addressed using a Lagrange multiplier formulation [10]. Defining λ_1, λ_2, and λ_3 as Lagrange multipliers, the constraint equations can be combined with cost function C to form a new cost function $\hat{C}$ which can be minimized in the usual unconstrained fashion:

$$\hat{C} = \frac{i' i}{\sqrt{i' B' B i}} + \sum_{j=1}^{3} \lambda_j \left[\frac{\gamma i' M_j i}{\sqrt{i' B' B i}} - f_j \right] \tag{24}$$

The coordinate transform

$$i = c\sqrt{c' B' B c} \tag{25}$$

simplifies the optimization problem considerably. Equation (24) written in terms of the new current vector c is

$$c' c + \sum_{j=1}^{3} \lambda_j (\gamma c' M_j c - f_j) \tag{26}$$

Conditions for an optimum are then

$$\begin{array}{lcl} c + \gamma(\lambda_1 M_1 + \lambda_2 M_2 + \lambda_3 M_3)\, c & = & 0 \\ \gamma c' M_1 c - f_1 & = & 0 \\ \gamma c' M_2 c - f_2 & = & 0 \\ \gamma c' M_3 c - f_3 & = & 0 \end{array} \tag{27}$$

Equations (27) are a set of 9 equations for 9 unknowns. This system can be solved for c and λ using a Newton-Raphson iteration [10].

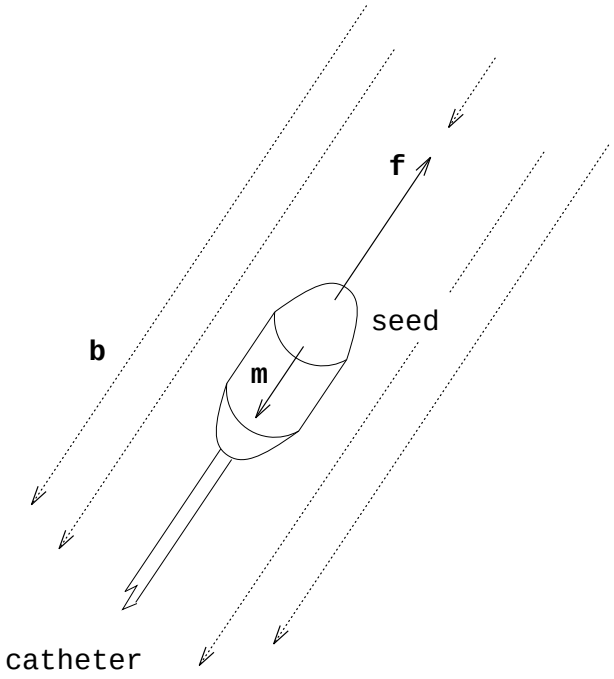

Figure 2: MSS seed in stable no-skid orientation.

5.2 No-Skid Seed

Again, it is required that **m** and **b** are parallel. The "no-skid" constraint additionally requires that the dipole must be stably aligned along the direction of motion. As a matter of convention, **m** is chosen to be anti-parallel to **f** in the stable configuration, implying that **b** should also be anti-parallel to **f**. This convention has been adopted because it matches the design of existing seeds used for pulling catheters in the MSS. However, the solution for the opposite convention is easily obtainable. The quadratic form of (22) guarantees that the same force is produced regardless of the sign of i. However, from (5), a change in the sign of i results in a reversal of field direction. The same force is produced, but the stable dipole orientation is rotated 180^o. Therefore, the negative of the solution under the present convention is the solution for the same force result with **m** stably oriented parallel to **b** rather than anti-parallel.

Without loss of generality, let $\mathbf{f}_d$ be a unit force in the desired force direction. If the seed is properly aligned,

$$\begin{array}{rcl} \mathbf{m} & = & -\gamma \mathbf{f}_d \\ \mathbf{b} & = & -\alpha \mathbf{f}_d \end{array} \tag{28}$$

where α is some presently unknown but positive real number, ensuring that the seed is stably aligned. This orientation is pictured in Figure 2. Further, from (9) and (5) we can substitute and form the following system of equations that is linear in i:

$$\left[\begin{array}{c} K(\mathbf{p}, -\gamma \mathbf{f}_d) \\ B(\mathbf{p}) \end{array} \right] i = \left\{ \begin{array}{c} f_d \\ -\alpha f_d \end{array} \right\} \tag{29}$$

or more concisely as

$$G\,i = d \quad \text{where} \quad G(\mathbf{p}, \mathbf{f}_d) = \left[\begin{array}{c} K(\mathbf{p}, -\gamma \mathbf{f}_d) \\ B(\mathbf{p}) \end{array} \right] \quad \text{and} \quad d(\alpha) = \left\{ \begin{array}{c} f_d \\ -\alpha f_d \end{array} \right\} \tag{30}$$

if the seed is properly aligned and the correct force is produced. For a given position specified by **p** and a desired force direction **f**, G is a uniquely determined 6×6 matrix. If G is nonsingular, the set of i that satisfies (29) is

$$i = G^{-1} d(\alpha) \tag{31}$$

However, an appropriate value for α has yet to be determined. The only constraint on α is that it must be positive so that the stable alignment of the seed matches the attitude assumed in (29) for forming K. (If α is negative, the stable orientation rotates by 180^o, changing the sign of the K matrix. The resulting force is then the opposite of the desired force.) Any arbitrary positive real α is a valid solution, but some solutions are more economical than others to realize. One way to choose α is such that α minimizes $i'i$ over the set of valid i. Equation (31) can be directly substituted into cost function $i'i$:

$$i'i = d(\alpha)'(G^{-1})'G^{-1}d(\alpha) \tag{32}$$

Equation (32) is a quadratic in one variable, α. The extremum of this quadratic must be a minimum since $i'i$ goes to $+\infty$ as α goes to $\pm\infty$.

Perhaps the simplest closed-form representation of the optimal α uses the singular value decomposition [11] of G:

$$G = UVW' \tag{33}$$

U and W are orthonormal matrices. V is a diagonal matrix whose entries are all greater than or equal to zero and are arranged in non-increasing order. The columns of U represent a basis for the output of Gi, and the diagonal entry corresponding to a column of U represents the inverse "cost" of realizing a unit output parallel to that column. Substituting (33) into (32) and minimizing with respect to α yields:

$$\alpha_{opt} = \frac{\begin{Bmatrix} f_d' & 0 \end{Bmatrix} UV^{-2}U' \begin{Bmatrix} 0 \\ f_d \end{Bmatrix}}{\begin{Bmatrix} 0 & f_d' \end{Bmatrix} UV^{-2}U' \begin{Bmatrix} 0 \\ f_d \end{Bmatrix}} \tag{34}$$

There is, however, no guarantee that α_{opt} is positive. Parameter α should then be chosen as

$$\alpha = \max[\alpha_{opt}, \alpha_{min}] \tag{35}$$

where α_{min} is an arbitrarily chosen minimum acceptable positive value, thereby ensuring that the dipole is properly oriented and adequately aligned.

In certain pathological cases, G is not invertible. These instances most often occur along lines of symmetry. For some of these cases, however, an answer satisfying (29) may still exist. With the singular value decomposition, (29) can be re-arranged as

$$VW'i = U'd(\alpha) \tag{36}$$

If G is of rank 5 rather than of rank 6 (and therefore singular), the last diagonal entry in V is zero. The cost to realize an output with any component along the last column of U is therefore infinite. For a solution to exist, α must be picked to satisfy the last equation in (36) (the vector d must be perpendicular to the unrealizable output vector):

$$0 = u'd(\alpha) \qquad \Rightarrow \qquad \alpha = \frac{u' \begin{Bmatrix} f_d \\ 0 \end{Bmatrix}}{u' \begin{Bmatrix} 0 \\ f_d \end{Bmatrix}} \tag{37}$$

where u is the last column of U. If (37) yields $\alpha > 0$, a solution that satisfies the no-skid conditions (and is perpendicular to the unrealizable space of outputs) exists. It is also interesting to note that α_{opt} (34) converges to (37) as G becomes singular.

In the singular case, there are multiple ways to produce any realizable output, since there is a six-dimensional space of inputs and a five- dimensional space of outputs. It can be shown that the most efficient way (in an $i'i$ sense) to produce the solution for the singular case is

$$i = WP\left[P'VP\right]^{-1}P'U'd(\alpha) \tag{38}$$

where P is the identity matrix with the last column removed and α satisfies (37).

5.3 Limited-Skid Seed

Under limited skid conditions, some misalignment between **m** and $-\mathbf{f}$ is considered acceptable. In this case, **b** is chosen so that the dipole is stably oriented at a small mis-alignment with **-f**. The desired **b** direction can be thought of as the direction of **f** rotated through some small angles about vectors perpendicular to **f**.

Define a new reference frame E such that

$$\left\{ \begin{array}{c} \mathbf{e}_1 \\ \mathbf{e}_2 \\ \mathbf{e}_3 \end{array} \right\} = T \left\{ \begin{array}{c} \mathbf{n}_1 \\ \mathbf{n}_2 \\ \mathbf{n}_3 \end{array} \right\} \text{ where } T = \left[\begin{array}{ccc} e_{11} & e_{12} & e_{13} \\ f_{d,1} & f_{d,2} & f_{d,3} \\ (e_{12} f_{d,3} - e_{13} f_{d,2}) & (e_{13} f_{d,1} - e_{11} f_{d,3}) & (e_{11} f_{d,2} - e_{12} f_{d,1}) \end{array} \right] \tag{39}$$

where $\mathbf{e}_1$ is some arbitrarily chosen unit vector such that

$$e_{11} f_{d,1} + e_{12} f_{d,2} + e_{13} f_{d,3} = 0 \tag{40}$$

Unit vectors $\mathbf{e}_1$ and $\mathbf{e}_3$ are perpendicular and $\mathbf{e}_2$ is parallel to the desired force direction. Define

$$\hat{\mathbf{f}}_d \equiv (-\sin\varepsilon_2)\mathbf{e}_1 + (\cos\varepsilon_1 \cos\varepsilon_2)\mathbf{e}_2 + (\sin\varepsilon_1 \cos\varepsilon_2)\mathbf{e}_3 \tag{41}$$

Angles ε_1 and ε_2 represent small rotations about $\mathbf{e}_1$ and $\mathbf{e}_3$ respectively. Vector $\hat{\mathbf{f}}_d$ is $\mathbf{f}_d$ misaligned by ε_1 and ε_2. With respect to the E frame:

$$\hat{f}_d(\varepsilon_1, \varepsilon_3) = T' \left\{ \begin{array}{c} -\sin\varepsilon_2 \\ \cos\varepsilon_1 \cos\varepsilon_2 \\ \sin\varepsilon_1 \cos\varepsilon_2 \end{array} \right\} \tag{42}$$

Instead of (28), the conditions now required are

$$\begin{array}{rcl} \mathbf{m} & = & -\gamma \hat{\mathbf{f}}_d \\ \mathbf{b} & = & -\alpha \hat{\mathbf{f}}_d \end{array} \tag{43}$$

so that the dipole is stably positioned and misaligned with $-\mathbf{f}_d$ by a small amount. These conditions imply the linear system

$$G i = \left\{ \begin{array}{c} f_d \\ -\alpha \hat{f}_d \end{array} \right\} \quad \text{where} \quad G(\mathbf{p}, \hat{\mathbf{f}}_d) = \left[\begin{array}{c} K(\mathbf{p}, -\gamma \hat{\mathbf{f}}_d) \\ B(\mathbf{p}) \end{array} \right] \tag{44}$$

The solutions for i and an appropriate α proceed exactly as for the no-skid case, given some arbitrary values of ε_1 and ε_2.

A convenient limit on the allowable skid is

$$\varepsilon_1^2 + \varepsilon_2^2 \leq \varepsilon_{max}^2 \tag{45}$$

where ε_{max} is the largest allowable skid angle. A search can then by made over the allowable region of ε's for the most economical solution.

6 Examples

As a demonstration of the above solutions, the procedures will be appled to the Magnetic Stereotaxis System (MSS). Since each problem is posed over a five-dimensional domain space of independent variables (consisting of seed location coordinates and two degrees of freedom to orient the force direction), an exhaustive comparison under all operating conditions is impractical. However, merely examining several randomly chosen points in the operating region is sufficient to reveal some of the character of each solution.

Before specific operating points can be tested, the general layout and specifications of the MSS must be described. This machine consists of six large superconducting coils arranged on the faces of a flattened cubical structure, as depicted in Figure 3. A right-handed coordinate system is defined as shown in the figure. Each axis of the coordinate system extends through the center of a pair of coils. The origin of the coordinate system is located at the center of the machine. Fluoroscopes for sensing seed position are aligned along the $X-$ and $Y-$axes, and the patient's head enters the machine along the $Z-$axis.

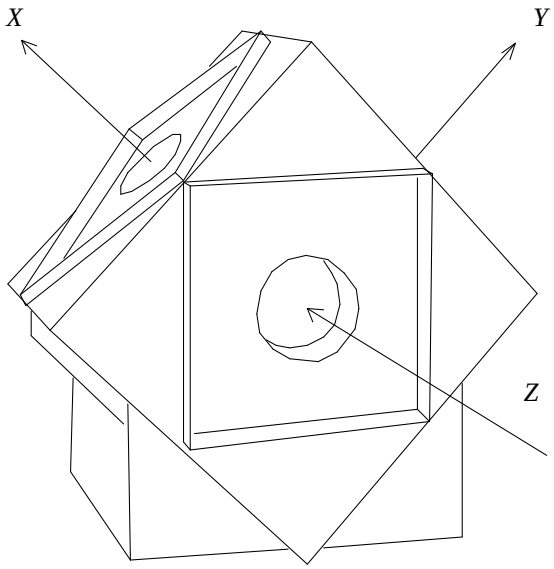

Figure 3: Magnetic Stereotaxis System.

Coil Dimensions

	X, Y axes	Z axis
Inner Dia.	28.00 cm	32.10 cm
Outer Dia.	37.20 cm	41.10 cm
Thickness	7.01 cm	3.72 cm
Distance between coil faces	45.69 cm	29.38 cm
turns/cm^2	207.2	207.2
Max. current	100 A	100 A

Table 1: MSS Coil Dimensions

Due to ergonomic constraints, the coils centered on the $X-$ and $Y-$axes are identical, whereas the two coils centered on the $Z-$axis are slightly flattened and closer together. The physical dimensions of these coils are given in Table 1. One seed employed in the MSS has a strength of 0.016 A$\cdot$m^2. This seed is a circular cylinder approximately 3 mm in diameter and 3 mm tall. Rounded plastic end pieces are usually attached to decrease resistance to seed motion. More detailed descriptions of the device, associated power electronics, and performance are contained in [2], [6] and [7].

The operating region of the MSS lies within a box that extends from -10 cm to 10 cm on the X- and Y-axes and from -14 cm to 6 cm on the Z-axis. Inside this region, a set of four random points and force directions have been chosen. Two more specifically chosen points are included because they represent interesting special cases where the G matrix is singular in the no-skid case: These points are summarized in Table 2.

For the no-skid and limited-skid cases, there is no *a priori* basis upon which to assume the the minimum acceptable value of α necessary to properly align the dipole. This value should most properly be determined experimentally. In the absence of these experimental results, α_{min} will be assumed zero arbitrarily, since this is the lowest possible value for maintaining a proper dipole alignment once that alignment is achieved.

#	Point			Force direction		
1	{ 1.50,	7.40,	-4.68}	{ -0.936,	0.338,	-0.094}
2	{ 2.88,	2.09,	-2.89}	{ 0.736,	-0.624,	0.259}
3	{ -5.78,	0.28,	-4.34}	{ -0.101,	-0.678,	-0.727}
4	{ 4.15,	-7.29,	6.79}	{ 0.456,	-0.234,	-0.858}
5	{ 5.00,	5.00,	0.00}	{ 0.707,	0.707,	0.00 }
6	{ -3.30,	-4.23,	5.04}	{ 0.506,	-0.046,	0.860 }

Table 2: Test points and desired force directions

	Currents, A/N						
#	-X	+X	-Y	+Y	-Z	+Z	α_{opt}
1.1	20161	20165	1389	13041	14300	15803	0.
1.2	-3847	4082	5616	-1675	-990	639	40.7
1.3	-3735	-5304	-3057	-3112	-2348	-1571	0.
1.4	6496	6580	5000	2805	2506	4002	0.
1.5	669	-16	669	-16	-1359	-1359	0.85
1.6	-	-	-	-	-	-	-4.18

Table 3: Coil currents, no-skid case.

6.1 No-Skid Case

Under the No-Skid conditions, currents are determined by solving the linear equation (29). The value of the arbitrary parameter α is chosen to be the greater of the α that minimizes (32) or α_{min}. Each of the points in Table 2 are considered under the No-Skid conditions, and the solution currents are summarized in Table 3. Examples (1.1-1.4) represent the typical solutions to (29). Example (1.1) is found to require enormously high currents, whereas other positions are less expensive. It is interesting to note that there is no particular propensity for α_{opt} as solved by (34) to turn out positive. In three of these examples, the arbitrary value of α_{min} has to be imposed for a properly aligned solution.

In examples (1.5) and (1.6), the G matrix of (29) is singular. These two are specifically chosen because (1.5) is a well-behaved singularity, and (1.6) is ill-behaved. Example (1.5) is typical of singularities in the MSS that arise from symmetry. These singularities occur when the seed is located on a plane of symmetry and the desired direction of motion is also within the plane of symmetry. In these cases, the G matrix is singular, but the unachievable space is perpendicular to all $d(\alpha)$ vectors, implying (37) is uniformly satisfied for all alpha. The choice of α is again arbitrary, and a good solution results. Example (1.6), however, does not yield a usable solution. When (37) is solved for the α that yields an answer perpendicular to the unachievable space, that α is negative – the only realizable alignment of the **b** vector with **f** has the wrong orientation.

If singularities such as (1.6) were a rare occurrence, a strategy would be to simply catalog and avoid them. However, this is not the case. Every point has some directions that are singular or badly conditioned in a MSS with six coils. For example, consider rotations of the desired force direction in (1.2). Let angles ε_1 and ε_2 represent rotation angles away from a nominal position, as detailed in Section 5.3. Figure 4 represents the 2-norm of the coil currents required to realize a no-skid force in the direction of (1.2) rotated by ε_1 and ε_2. From this figure, it is evident that even though the specific direction considered in (1.2) is nonsingular and well-behaved, many other possible force directions produced from the same point are very badly behaved.

6.2 Limited-Skid Case

For the limited-skid case, a mis-alignment of up to 20^o is arbitrarily deemed tolerable. Under the Limited-Skid conditions, currents are determined by solving (44) on a fine grid of perturbed seed orientations inside the allowable skid region. At any particular seed orientation, the solution only requires the inversion of a

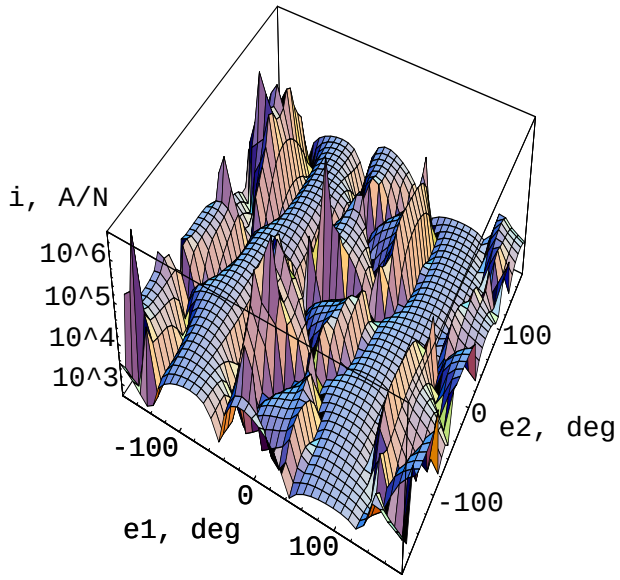

Figure 4: 2-norm of coil currents versus force orientation for example 1.2.

	Currents, A/N							
#	-X	+X	-Y	+Y	-Z	+Z	α_{opt}	ε
2.1	1196	855	856	191	-477	-1717	0.	19.9^o
2.2	-431	1068	1721	154	-778	-1671	8.05	19.9^o
2.3	-610	-2755	971	730	441	917	0.94	8.49^o
2.4	3052	2709	1533	-1073	1994	1698	0.	18.04^o
2.5	669	-16	669	-16	-1360	-1360	0.85	$0.^o$
2.6	600	1282	-574	-2089	1214	577	0.97	8.94^o

Table 4: Coil currents, limited skid case.

6×6 matrix. At each orientation, the value of the arbitrary parameter α is chosen to be the greater of the α that minimizes (32) or α_{min}. The orientation with the lowest required $i'i$ is then chosen as the solution. Each of the seed location and force direction pairs in Table 2 is considered under the Limited-Skid conditions, and the solution currents are summarized in Table 4.

In general, there is a marked improvement in the current levels required for a given force. For instance, example (2.1), shows an order-of-magnitude decrease in the peak required current. The other examples exhibit a similar improvement in performance. Only (2.5) remains unchanged; the locally most efficient orientation is the no-skid orientation for this particular example. Of special note is example (2.6). In the no-skid configuration, no solution existed. With less than 10^o of mis-alignment, however, this example has a fairly economical solution.

The improvements in solution economy rely on the fact that economical orientations are often quite close to orientations that are prohibitively expensive to realize. In the particular case of (2.1), the no-skid solution is quite expensive. In Figure 5, it can be seen that the no-skid orientation (at the center of the figure) lies very close to a ridge of singularities. By allowing mis-alignment, an attitude at the far edge of the figure and away from the singularities is used.

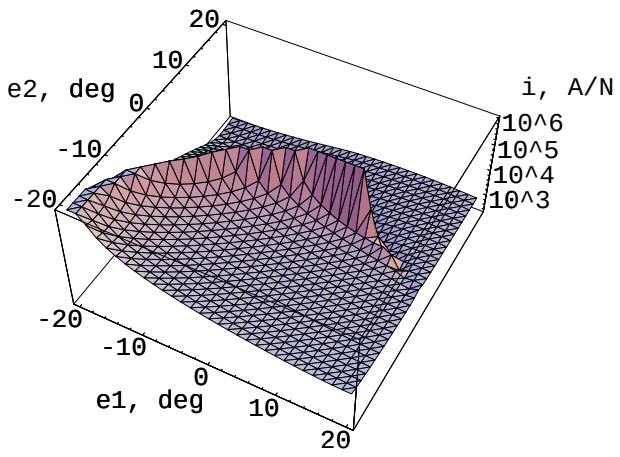

Figure 5: 2-norm of coil currents versus dipole orientation for example 2.1.

	Currents, A/N							
#	-X	+X	-Y	+Y	-Z	+Z	α_{opt}	ε
3.1	-1832	-273	69	1116	1025	226	9.73	90.58^o
3.2	135	-1442	1334	-251	-226	2290	9.08	103.68^o
3.3	362	-298	1537	-277	-953	-784	8.69	83.75^o
3.4	-1132	942	-1423	993	2210	-724	16.78	57.81^o
3.5	-31	-849	31	849	0.	0.	8.09	$90.^o$
3.6	-459	1439	254	-297	91	-1186	10.8	118.02^o

Table 5: Coil currents, unlimited skid case.

6.3 Unlimited-Skid Case

The dipole orientation will now be considered unconstrained. Instead of simply solving linear equations, the unconstrained dipole orientation requires the solution of (27). A Newton-Raphson iteration starting from a randomly chosen set of currents was used to solve this equation. There are typically a finite number of local minima (usually about five) to which this iteration can converge, so the iteration was run several times to ensure a global minimum. The results for this scenario corresponding to the test points in Table 2 are summarized in Table 5.

As with the limited-skid case, the unlimited skid case produced a valid result for each case. The current magnitudes are roughly equivalent to the results of the limited-skid case, but each example now has an α of around 10; to realize these α_{min} of 10 in the limited skid case would increase the required current magnitudes, possibly considerably.

A similar solution to the unlimited skid case would be obtained by applying the limited-skid conditions over ε's ranging from -180^o to 180^o. The value of α_{min} would again be explicitly chosen, an option that does not exist in the quadratic formulation.

7 Conclusions

Three types of solution have been presented for the purpose of applying an arbitrary force to the magnetic dipole in a magnetic stereotaxis system. The no-skid case, assuming that the force and dipole moment were anti-parallel, required large currents. The no-skid constraint is overly restrictive and leads to problems with singularities arising from coil placement. The limited-skid case, however, is able to solve for currents away

from the singularities by tolerating an error in alignment. A large reduction in required currents was observed in the specific examples considered. Likewise, the unlimited skid case allows an arbitrary degree of misalignment. Current levels in test examples were roughly equal to those of the limited-skid case, but the dipole alignment was much stronger in the unlimited skid case.

There are some further considerations about which particular set of alignment constraints to implement in a working magnetic stereotaxis system. For use in hyperthermia treatments (where there is no catheter), the best approach might be to use a spherical seed (such that there is no preferential orientation) and choose forces by either the limited-skid or unlimited skid conditions. The catheter placement mission, however, has additional complicating factors. For example, the catheter may be so stiff as to prevent correct alignment of the dipole with the field. Additionally, it is not guaranteed that the skid-attitude of a capsule-shaped seed would remain constant during motion. Contact forces from the brain tissue might deflect the seed and change the resulting force direction.

Some of the above limitations might be addressed with design changes in the MSS. For example, operating in the no-skid mode may be possible if the MSS were built of many small coils rather than just six large coils. If this were the case, the G matrix would contain extra columns and would be inverted using a Moore-Penrose pseudoinverse [11] in (31). The chances of encountering a pathological condition that would reduce the rank of G to 5 would then be much lower. Likewise, individual coil currents would go down because there would be more coils acting in concert to produce the force.

For the cases allowing skid, a catheter tip with a universal joint would allow an arbitrary skid without interference from the catheter or from contact forces. The fabrication of such a device might be, however, a considerable problem in itself.

Several other theoretical issues remain to be considered in future work. The present work has considered only static forces produced at a point in the helmet; the time-based problem of optimizing currents with the goal of minimizing quench risk has yet to be considered. In addition, the optimality of the present approach is only point-wise; although each point on a trajectory is optimized, it may be that there are alternate trajectories that are much cheaper in the sense of transit time with adequate quench safety margin.

References

[1] J. A. Molloy *et al.*, "Thermodynamics of moveable inductively heated seeds for the treatment of brain tumors," *Medical Physics*, vol. 18. pp. 794-803, 1991.

[2] G. T. Gillies *et al.*, "Magnetic manipulation instrumentation for medical physics research," *Rev. Sci. Inst.*, vol. 65, no. 3, pp. 533-562, 1994.

[3] R. C. Ritter *et al.*, "Magnetic stereotaxis: computer-assisted, image-guided remote movement of implants in the brain," *Innovation et Technologie en Biologie et Medecine*, vol. 13. pp. 437-449, 1992.

[4] M. S. Grady, M.D. *et al.*, "Nonlinear magnetic stereotaxis: three-dimensional, in vivo remote magnetic manipulation of a small object in canine brain," *Medical Physics*, vol. 17. pp. 405-415, 1990.

[5] E. G. Quate *et al.*, "Goniometric motion controller for the superconducting coil in a magnetic stereotaxis system," *IEEE Trans. Bio. Engr.*, vol. 38, pp. 899-905, 1991.

[6] R. G. McNeil *et al.*, "Functional design features and initial performance characteristics of a magnetic implant guidance system for stereotactic neurosurgery," *IEEE Trans. Bio. Engr.*, vol. 42, pp. 793-801, 1995.

[7] R. G. McNeil *et al.*, "Characteristics of an improved magnetic-implant guidance system," *IEEE Trans. Bio. Engr.*, vol. 42, pp. 802-808, 1995.

[8] J. D. Jackson, *Classical Electrodynamics*, 2^{nd} ed., New York: Wiley, 1975.

[9] S. R. Hoole, *Computer-Aided Analysis and Design of Electromagnetic Devices*, New York: Elsevier, 1989.

[10] R. L. Fox, *Optimization Methods for Engineering Design*, Reading, MA: Addison-Wesley, 1971.

[11] R. A. Horn and C. R. Johnson, *Matrix Analysis*, New York: Cambridge University Press, 1985.